

# The Effect of Clock, Media, and Station Location Errors On Doppler Measurement Accuracy

J. K. Miller  
Navigation Systems Section

*Doppler tracking by the DSN is the primary radio metric data type used by navigation to determine the orbit of a spacecraft. The accuracy normally attributed to orbits determined exclusively with Doppler data is about 0.5 microradians in geocentric angle. Recently, the Doppler measurement system has evolved to a high degree of precision primarily because of tracking at X-band frequencies (7.2 to 8.5 GHz). However, the orbit determination system has not been able to fully utilize this improved measurement accuracy because of calibration errors associated with transmission media, the location of tracking stations on the Earth's surface, the orientation of the Earth as an observing platform, and timekeeping. With the introduction of Global Positioning System (GPS) data, it may be possible to remove a significant error associated with the troposphere. In this article, the effect of various calibration errors associated with transmission media, Earth platform parameters, and clocks are examined. With the introduction of GPS calibrations, it is predicted that a Doppler tracking accuracy of 0.05 microradians is achievable.*

## I. Introduction

The Doppler data type provides a measure of the line-of-sight range rate between a tracking station and a spacecraft. This functional definition is useful for analyzing orbit determination errors that are spacecraft or trajectory dependent, but is of little use for analyzing error sources close to the actual measurement such as media or instrumentation errors. The actual measurement is a count of a signal derived from the signal received from the spacecraft and a frequency standard maintained at the tracking station that is related to the transmitted signal. Thus, a precision model of the Doppler observable would include

a model of the signal path and hardware elements as well as spacecraft dynamics. In practice, the instrumentation errors are small compared to media, station location, and spacecraft dynamics errors and, therefore, a simple functional model of the hardware should suffice.

A model of the Doppler observable is developed below that idealizes some of the instrumentation error sources yet precisely models the external environment. This model is sufficiently precise for computation of the observable and is essentially the model contained in JPL's Orbit Determination Program (ODP) [1]. Of particular interest are models

that are external to the DSN tracking station hardware, yet pertain directly to the signal path. Media effects and the effect of general relativity on the station clocks are examples. Other models, such as station locations and polar motion, though not directly part of the Doppler measurement system, are treated as measurement calibrations for the purposes of analysis and orbit determination.

## II. Doppler Measurement Model

The Doppler measurement is simply an electronic count of the number of cycles from a frequency standard ( $N_c$ ) minus the number of cycles of the spacecraft signal received by the ground station ( $N_r$ ), scaled by the count time interval ( $\Delta T_c$ ). Thus

$$Z_m = \frac{(N_c - N_r) + n}{\Delta T_c} \quad (1)$$

where  $n$  is the measurement noise, which is typically about 1/10 of a cycle. The received frequency and standard frequency need not be counted individually and differenced, but are added together electronically and the beat frequency counted. This is a detail that is dependent on the hardware implementation. The numerical value of  $Z_m$  is the number that is recorded on the tracking data file and is sent to the ODP for orbit determination; the units of  $Z_m$  are hertz.

In the ODP, one needs to obtain a computed value for  $Z_m$  as a function of parameters that are available to the ODP. This function can be derived from the equations of motion and the physical model of the system or can be worked backwards from Eq. (1) for the measurement. Working backwards from the measurement equation is chosen because the starting point is an equation that represents the real physical measurement.

The frequency standard is obtained by scaling the reference oscillator frequency ( $f_q$ ) to equal the transmitted frequency times the spacecraft turnaround ratio which would nominally be the received frequency if there were no spacecraft Doppler shift or additional delay.

$$N_c = C_3 f_t \Delta T_c \quad (2)$$

where for S-band (2.1 to 2.3 GHz) Doppler,

$$C_3 = \frac{240}{221}$$

$$f_t = 96 f_q$$

$$\Delta T_c = T_{3e} - T_{3s}$$

The count time ( $\Delta T_c$ ) is defined as the difference between the reception time at the start of the count-time interval ( $T_{3s}$ ) and the reception time at the end of the interval ( $T_{3e}$ ). For a schematic representation of these times, see Fig. 1. In Eq. (2), all the parameters are constant or arbitrarily specified, including the reception times. The real information content of the measurement is contained within the count  $N_r$ . Thus, to obtain a complete equation for the computed measurement, one needs an equation for  $N_r$ . It is tempting to differentiate and work in the frequency domain; however, the actual observable is accumulated phase change, and this is a sufficient reason to keep this representation. Therefore, it is necessary to formulate the data type in terms of phase thus bypassing an explicit equation for the received frequency. The equation that relates the measurement to the observable parameters is simply

$$N_r = C_3 N_t \quad (3)$$

where

$$N_t = f_t (T_{1e} - T_{1s})$$

Equation (3) for  $N_r$  states that the number of cycles counted at the receiver is equal to the number of cycles transmitted ( $N_t$ ) times the spacecraft turnaround ratio. This equation is true because the transmitted cycles are effectively the same as the received cycles. Thus, the information content of the measurement is now contained in the transmit times  $T_{1e}$  and  $T_{1s}$ . Since both of these times are unknown, some additional equations are needed to tie into the observable quantities. At this point in the development, the following equation for the computed measurement is introduced:

$$Z_c = (T_{3e} - T_{3s} - T_{1e} + T_{1s}) \frac{C_3 f_t}{\Delta T_c} \quad (4)$$

Equations are needed for the times in Eq. (4) and these will be developed as functions of ephemeris time  $t$ . The equation for the atomic clock at the station is

$$T = t + F(t, x, y) \quad (5)$$

where  $x$  refers to state variables and  $y$  refers to various constant parameters.

The station time ( $T$ ) is equal to the ephemeris time  $t$  modified by a small correction because of relativity and any other parameter that may affect the running of the clock. The calibration function ( $F$ ) is a function of time, the solar system gravitational potential, and other constant parameters. The relevant times relating to the Doppler measurement are

$$T_{1s} = t_{1s} + F(t_{1s}, x, y)$$

$$T_{1e} = t_{1e} + F(t_{1e}, x, y)$$

$$T_{3s} = t_{3s} + F(t_{3s}, x, y)$$

$$T_{3e} = t_{3e} + F(t_{3e}, x, y)$$

Making the above substitutions, the equation for the computed observable becomes

$$\begin{aligned} Z_c = & (t_{3e} - t_{3s} - t_{1e} + t_{1s}) \frac{C_3 f_t}{\Delta T_c} \\ & + [F(t_{3e}, x, y) - F(t_{3s}, x, y) - F(t_{1e}, x, y) \\ & + F(t_{1s}, x, y)] \frac{C_3 f_t}{\Delta T_c} \end{aligned} \quad (6)$$

Since the speed of light is constant in any reference frame, one obtains, by integrating along the light path,

$$t_{3e} - t_{1e} = \frac{\rho_{12e} + \rho_{23e}}{c} + \Delta t_{1e}^m + \Delta t_{3e}^m \quad (7)$$

$$t_{3s} - t_{1s} = \frac{\rho_{12s} + \rho_{23s}}{c} + \Delta t_{1s}^m + \Delta t_{3s}^m \quad (8)$$

where the  $\rho$  terms represent the integrated distance along the light path and the  $t^m$  terms represent the additional delay caused by transmission media. The distances along the light path,

$$\rho_{12s} = \int \int_{t_{1s}}^{t_{2s}} \ddot{\rho} dt dt \quad (9)$$

$$\rho_{23s} = \int \int_{t_{2s}}^{t_{3s}} \ddot{\rho} dt dt \quad (10)$$

$$\rho_{12e} = \int \int_{t_{1e}}^{t_{2e}} \ddot{\rho} dt dt \quad (11)$$

$$\rho_{12e} = \int \int_{t_{2e}}^{t_{3e}} \ddot{\rho} dt dt \quad (12)$$

are obtained by integrating the equations of motion for the spacecraft. These equations are referred to as the light time equations and are solved iteratively for the arguments of integration. The media delay is included in the measurement equation by evaluating the calibration function ( $G$ ) at the appropriate times:

$$\Delta t^m = G(t, x, y) \quad (13)$$

and

$$\Delta t_{1s}^m = G(t_{1s}, x, y)$$

$$\Delta t_{1e}^m = G(t_{1e}, x, y)$$

$$\Delta t_{3s}^m = G(t_{3s}, x, y)$$

$$\Delta t_{3e}^m = G(t_{3e}, x, y)$$

The final equation [Eq. (14)] for  $Z_c$  (the computed measurement) includes the observable equations as well as clock and media calibration functions:

$$\begin{aligned} Z_c = & \frac{\rho_{12e} + \rho_{23e} - \rho_{12s} - \rho_{23s}}{c} \frac{C_3 f_t}{\Delta T_c} \\ & + [F(t_{3e}, x, y) - F(t_{3s}, x, y) - F(t_{1e}, x, y) \\ & + F(t_{1s}, x, y)] \frac{C_3 f_t}{\Delta T_c} + [G(t_{3e}, x, y) - G(t_{3s}, x, y) \\ & + G(t_{1e}, x, y) - G(t_{1s}, x, y)] \frac{C_3 f_t}{\Delta T_c} \end{aligned} \quad (14)$$

### III. Analytic Doppler Error Model

Equation (14) for the computed measurement, while useful for actual orbit determination operations, is somewhat cumbersome for error analysis. An error analysis could be performed by combining the sensitivities of each term in Eq. (14). An alternative method would be to develop an approximate analytic representation of the computed measurement which will be pursued below. The range from the tracking station to the spacecraft may be described by the following function obtained by integrating the equations of motion:

$$\rho = R(t, x, y) \quad (15)$$

The velocity of the spacecraft projected along the Earth line of sight is obtained by differentiating the range and is given by

$$\dot{\rho} = \frac{\partial R}{\partial t} \quad (16)$$

which may be approximated by

$$\dot{\rho} \approx \frac{R(t_e, x, y) - R(t_s, x, y)}{\Delta T_c} \quad (17)$$

From the geometry shown on Fig. 1, then

$$R(t_e, x, y) - R(t_s, x, y) = \frac{1}{2} (\rho_{12e} + \rho_{23e} - \rho_{12s} - \rho_{23s}) \quad (18)$$

Substituting Eq. (18) into the equation for the measurement, the following expression is obtained for the geometric part of the computed measurement:

$$Z_c \approx \frac{2 C_3 f_t}{c} \frac{\partial R}{\partial t} \quad (19)$$

Consider the following generic function for the clock and media calibration functions:

$$Z = F(t) \quad (20)$$

For small  $\Delta t$ , the second derivative may be approximated by

$$\frac{\partial^2 Z}{\partial t^2} = \frac{F(t + 2\Delta t) - 2F(t + \Delta t) + F(t)}{\Delta t^2} \quad (21)$$

In the limit as  $\Delta t$  approaches zero, this is the definition of the second derivative. Without loss of generality, one can evaluate the second derivative using two separate  $\Delta t$ 's (one for the first derivative and the other for the second derivative)

$$\begin{aligned} \frac{\partial^2 Z}{\partial t^2} &= \frac{F(t + \Delta t_2 + \Delta t_1) - F(t + \Delta t_2)}{\Delta t_1 \Delta t_2} \\ &\quad - \frac{F(t + \Delta t_1) - F(t)}{\Delta t_1 \Delta t_2} \end{aligned} \quad (22)$$

Solving for the values of the function at the indicated times and rearranging the terms gives

$$\begin{aligned} F(t + \Delta t_1 + \Delta t_2) - F(t + \Delta t_2) - F(t + \Delta t_1) \\ + F(t) = \frac{\partial^2 Z}{\partial t^2} \Delta t_1 \Delta t_2 \end{aligned} \quad (23)$$

If one makes  $\Delta t_1$  equal to the count time ( $\Delta T_c$ ) and  $\Delta t_2$  equal to the round-trip light time ( $\Delta t_{rtl}$ ), the above calibrations can be approximated by the second derivative of the calibration function, provided this function has frequency components with periods that are long compared to the delta times. Thus, for the clock calibration function evaluations,

$$F(t_{3e}) - F(t_{3s}) - F(t_{1e}) + F(t_{1s}) \approx \frac{\partial^2 F(t)}{\partial t^2} \Delta T_c \Delta t_{rtl} \quad (24)$$

For the media calibration function, one may perform a similar approximation. However, because of the reversal of signs in Eq. (14), the dominant term is given by the first derivative and then

$$G(t_{3e}) - G(t_{3s}) + G(t_{1e}) - G(t_{1s}) \approx 2 \frac{\partial G(t_{1e})}{\partial t} \Delta T_c \quad (25)$$

Substituting into the exact equation for the measurement gives the following approximation:

$$Z_m \approx C_3 f_t \left[ \frac{2\dot{\rho}}{c} + \frac{\partial^2 F(t)}{\partial t^2} \Delta t_{rtl} + 2 \frac{\partial G(t_{1e})}{\partial t} \right] \quad (26)$$

However, if the round-trip light time is too long relative to the count time, as would be the case for the outer planets, then

$$Z_m \approx C_3 f_t \left[ \frac{2\dot{\rho}}{c} + \frac{\partial F(t_3, x, y)}{\partial t} - \frac{\partial F(t_1, x, y)}{\partial t} + \frac{\partial G(t_3, x, y)}{\partial t} + \frac{\partial G(t_1, x, y)}{\partial t} \right] \quad (27)$$

The evaluation of the partial derivatives is greatly facilitated by breaking up the calibration functions into individual terms and approximating with simple functions (preferably sines, cosines, or exponentials). The sensitivity of the measurement to various  $y$  parameters that are used to describe the calibration functions is given by

$$\Delta Z_m \approx C_3 f_t \left[ 2 \frac{\partial^2 R(t, x, y)}{\partial y \partial t} + 2 \frac{\partial^2 G(t, x, y)}{\partial y \partial t} + \frac{\partial^3 F(t, x, y)}{\partial y \partial t^2} \Delta t_{rtl} \right] \Delta y \quad (28)$$

The  $y$  parameters in Eq. (28) can be formed into a covariance matrix which, when pre- and post-multiplied by the measurement sensitivities, gives the measurement variance.

For example, consider the case where the only  $y$  parameter is the amplitude of the daily special relativity term that is part of the atomic clock calibration function. This term is defined by

$$F_e = \alpha_e r_s \sin(\omega_e t + \lambda_s + \phi) \quad (29)$$

where  $\alpha_e$  is the subject  $y$  parameter,  $r_s$  is the station spin radius,  $\omega_e$  is the Earth rotation rate,  $\lambda_s$  is the tracking station longitude, and  $\phi$  is a phase angle needed to bring UT1 into agreement with ephemeris time. Typical nominal values of these parameters are given by

$$\alpha_e = 3.17679 \times 10^{-10} \text{ sec/km}$$

$$r_s = 5,204 \text{ km}$$

$$\omega_e = 7.292 \times 10^{-5} \text{ rad/sec}$$

Taking the required first and second partial derivatives, one obtains the following equation for the measurement error as a function of time:

$$\sigma_z \approx |C_3 f_t \Delta t_{rtl} r_s \omega_e^2 \sin(\omega_e t + \lambda_s + \phi)| \sigma_{\alpha_e} \quad (30)$$

where, at X-band and for a typical round-trip light time,

$$T_{rtl} = 1,512 \text{ sec}$$

$$C_3 = \frac{880}{749}$$

$$f_t = 32 f_q + 0.65 \times 10^{10} \text{ Hz}$$

$$f_q = 20.98 \times 10^6 \text{ Hz}$$

$$\sigma_{\alpha_e} = 3.17679 \times 10^{-10} \text{ sec/km}$$

This equation gives a peak amplitude of 70 mHz for a 100-percent error in the amplitude ( $\alpha_e$ ). Thus, to obtain a 1-mHz accuracy in the measurement, the calibration error must be less than 2 percent.

## IV. Data Noise Evaluation

Approximately two orbits of Magellan data were processed from February 7, 1991, 19:29:02 (ET) to February 8, 1991, 00:10:33 (ET). The postfit residuals are shown on Fig. 2, which involved solving for the spacecraft state, a constant nongravitational acceleration, and a fourth-degree and -order spherical harmonic gravity field. The first 10,000 sec of data shown on Fig. 2 are from Deep Space Station (DSS) 15. The gap around 6,000 sec is data unavailable near periapsis. Data after 12,000 sec are from DSS 45.

Recall from Eq. (1) that the measurement noise is

$$Z_m = \frac{N_c - N_r}{\Delta T_c} + \frac{n}{\Delta T_c} \quad (31)$$

The data noise is approximately 1/10 of a cycle count, and is independent of frequency. For a 60-sec count time, the Doppler data noise is therefore about 1.66 mHz. This value agrees with Fig. 2, which shows noise of this magnitude from DSS 15 and appears to be uniformly distributed but with some structure. The data from DSS 45 are a bit more noisy and appear more Gaussian.

Doppler data are scaled by the count time to make the recorded measurement proportional to range rate. The

Doppler measurement sensitivity to line-of-sight velocity is given by Eq. (19):

$$Z_{\dot{\rho}} \approx \frac{2C_3 f_t}{c} \dot{\rho} \quad (32)$$

At S-band, typical values for the constants in the above equation are:

$$C_3 = \frac{240}{221}$$

$$f_t = 96 f_q$$

$$f_q = 22 \times 10^6 \text{ Hz}$$

$$c = 299792.458 \text{ km/sec}$$

and solving Eq. (32) for  $\dot{\rho}$  gives 0.108 mm/sec for  $Z_{\dot{\rho}} = 1.66 \text{ mHz}$  data noise. One can also obtain from Eq. (32) the well-known result that for  $\dot{\rho} = 1 \text{ mm/sec}$  the measurement noise is  $Z_{\dot{\rho}} = 15.3 \text{ mHz}$ . At X-band, the measurement noise  $Z_{\dot{\rho}} = 1.66 \text{ mHz}$  corresponds to 0.03 mm/sec velocity.

## V. Troposphere Calibration

A radio signal passing through the Earth's troposphere will be delayed depending on the dielectric constant of the media and path length. A functional formula for this delay has been defined above.

$$\Delta t^t = G_t(t, x, y) \quad (33)$$

The sensitivity of the Doppler measurement to media is functionally given by Eq. (28) and one may extract the part that pertains to the troposphere.

$$\Delta Z_m \approx 2C_3 f_t \frac{\partial^2 G_t(t, x, y)}{\partial y \partial t} \Delta y \quad (34)$$

The troposphere delay has been separated into wet and dry components that are functions of delay at zenith ( $z$ ) and elevation angle ( $\gamma$ ):

$$G_t(t, x, y) = R_d + R_w \quad (35)$$

$$R_d = f_d(z_d, \gamma) \quad (36)$$

$$z_d = f_{z_d}(t, y) \quad (37)$$

$$R_w = f_w(z_w, \gamma) \quad (38)$$

$$z_w = f_{z_w}(t, y) \quad (39)$$

$$\gamma = f_{\gamma}(t) \quad (40)$$

In taking the required partial derivatives with respect to time, one assumes  $R_w$  and  $R_d$  are linear in  $z_w$  and  $z_d$  and  $\gamma$  is a function of only time:

$$\frac{\partial G_t}{\partial t} = \frac{\partial R_d}{\partial \gamma} \dot{\gamma} + \frac{\partial R_d}{\partial z_d} \frac{\partial z_d}{\partial t} + \frac{\partial R_w}{\partial \gamma} \dot{\gamma} + \frac{\partial R_w}{\partial z_w} \frac{\partial z_w}{\partial t} \quad (41)$$

The expression for the measurement sensitivity becomes

$$\Delta Z_m \approx 2C_3 f_t \left[ \frac{\partial^2 R_d}{\partial y \partial \gamma} \dot{\gamma} + \frac{\partial R_d}{\partial z_d} \frac{\partial^2 z_d}{\partial y \partial t} + \frac{\partial^2 R_w}{\partial y \partial \gamma} \dot{\gamma} + \frac{\partial R_w}{\partial z_w} \frac{\partial^2 z_w}{\partial y \partial t} \right] \Delta y \quad (42)$$

The first term in the above equation represents the non-linearity of the dry troposphere mapping function, and the second term represents the variation in the dry troposphere  $z$  height due to local weather. The next two terms are the same quantities for the wet troposphere. The troposphere wet and dry mapping functions are tabulated as delay as a function of spacecraft elevation angle. Empirical formulas for these mapping functions are given by [2,3]

$$R_d = \frac{1}{C} \frac{z_d}{\sin \gamma + \frac{A_d}{B_d + \tan \gamma}} \quad (43)$$

$$R_w = \frac{1}{C} \frac{z_w}{\sin \gamma + \frac{A_w}{B_w + \tan \gamma}} \quad (44)$$

where

$$\sin \gamma = \cos \delta \cos \lambda \cos \phi + \sin \lambda \cos \phi + \sin \phi \sin \delta \quad (45)$$

$$\lambda = \omega_e t + \lambda_s - \alpha \quad (46)$$

The dry component of the troposphere ( $R_d$ ) is a function of the delay at zenith ( $z_d$ ), the elevation angle ( $\gamma$ ), and constants  $A_d$  and  $B_d$  that are provided to model the bending at low-elevation angles. The wet component ( $R_w$ ) is similarly defined. The elevation angle ( $\gamma$ ) is computed as a function of the latitude of the tracking station ( $\phi$ ), the declination of the spacecraft ( $\delta$ ), and the local hour angle with respect to the spacecraft ( $\lambda$ ). The local hour angle is zero when the spacecraft is at zenith and is a function of the Greenwich hour angle ( $\omega_e t$ ), the station longitude ( $\lambda_s$ ), and the right ascension of the spacecraft ( $\alpha$ ).

The dry component of the troposphere is assumed to be stable and most of the variability is associated with the wet component. The variation in the wet component may be modeled as a periodic variation in the  $z$  height ( $z_w$ ). The actual variation obtained by tracking the GPS satellites in early 1991 is shown on Fig. 3. The hourly variation in the wet component of the troposphere appears as a random walk that would require a high-order Fourier series to represent analytically. For the purpose of error analysis, the variation may be modeled as a simple sinusoid with amplitude and frequency selected to be representative of Fig. 3.

$$z_w = z_{w0} + z_{w1} \sin(\omega_{w1} t) \quad (47)$$

For the troposphere, the  $y$  parameters that are of interest are the constant coefficient of the wet  $z$  height function ( $z_{w0}$ ) and the periodic coefficient ( $z_{w1}$ ). In order to obtain these sensitivities, it is necessary to evaluate the partial derivatives contained in the above measurement sensitivity function [Eq. (59)] that pertain to the wet troposphere component. For elevation angles above the horizon by a few degrees, one can approximate the mapping function by

$$R_w \approx \frac{1}{c} \frac{z_w}{\sin \gamma} \quad (48)$$

and

$$\frac{\partial R_w}{\partial \gamma} = \frac{1}{c} \frac{-z_w \cos \gamma}{\sin^2 \gamma} \quad (49)$$

$$\frac{\partial R_w}{\partial z_w} = \frac{1}{c} \frac{1}{\sin \gamma} \quad (50)$$

The partial derivatives of  $\gamma$  and  $z_w$  with respect to time are given by

$$\dot{\gamma} = \frac{\cos \phi (\cos \lambda - \cos \delta \sin \lambda)}{\cos \gamma} \dot{\lambda} \quad (51)$$

$$\dot{\lambda} = \omega_e \quad (52)$$

$$\dot{z}_w = z_{w1} \omega_{w1} \cos(\omega_{w1} t) \quad (53)$$

One is interested in the sensitivity of the Doppler measurement to the constant and periodic terms of the expression for the wet troposphere  $z$  height:

$$\Delta Z_m \approx \frac{2C_3 f_t}{c} \frac{\partial^2 R_w}{\partial y \partial \gamma} \dot{\gamma} \Delta y \quad (54)$$

Substituting the above partial derivatives into this equation yields

$$\Delta Z_{z_0} \approx \frac{2C_3 f_t}{c} \frac{\cos \gamma}{\sin^2 \gamma} \dot{\gamma} \Delta z_{w0} \quad (55)$$

and so

$$\begin{aligned} \Delta Z_{z_1} &\approx \frac{2C_3 f_t}{c} \\ &\times \left\{ \frac{1}{\sin \gamma} \omega_{w1} \cos \omega_{w1} t - \frac{\cos \gamma}{\sin^2 \gamma} \dot{\gamma} \sin \omega_{w1} t \right\} \Delta z_{w1} \end{aligned} \quad (56)$$

An example of the effect of the troposphere on X-band Doppler is the application of GPS troposphere calibration data to the Magellan spacecraft. The GPS data were obtained at a time when the spacecraft was in orbit about Venus. It would be preferable to have cruise data, where the effect of the troposphere is more pronounced, rather than orbiting data where separation of the tropospheric effect from the gravity field modelling effects is difficult. Recall the two orbits of Magellan Doppler residuals shown on Fig. 2. At the time of the first data point, the parameters in the above Doppler sensitivity equations had the following values:

$$C_3 = \frac{880}{749}$$

$$\gamma = 37.49 \text{ deg}$$

$$f_i = 32f_q + 0.65 \times 10^{10} \text{ Hz}$$

$$\dot{\gamma} = 3.818 \times 10^{-5} \text{ rad/sec}$$

$$f_q = 20.98 \times 10^6 \text{ Hz}$$

$$z_{w0} = 5 \times 10^{-5} \text{ km}$$

$$z_{w1} = 5 \times 10^{-5} \text{ km}$$

$$\omega_{w1} = 1.454 \times 10^{-4} \text{ rad/sec}$$

The above analytic Doppler sensitivity equations reveal a Doppler measurement error sensitivity of 0.044 mHz per centimeter of constant wet troposphere  $z$  height ( $z_{w0}$ ) error and a periodic Doppler measurement sensitivity of 0.044 mHz in quadrature with 0.134 mHz per centimeter of variable wet troposphere  $z$  height amplitude ( $z_{w1}$ ). Figure 4 shows the prefit residuals for the periodic wet troposphere  $z$  height calibration defined above. A Doppler shift of about 0.67 mHz is apparent early on for the data from DSS 15; at the end of Fig. 4, the Doppler shift is about 2 mHz for the low elevation data from DSS 45. The data in Fig. 4 indicate that the error contribution of the troposphere, which may amount to several mHz, could be reduced or eliminated with GPS calibration data.

## VI. Ionosphere Calibration

A radio signal passing through the ionosphere experiences a reduction in group velocity and an equal increase in phase velocity that is a function of the frequency and the number of charged particles along the signal path. The Doppler measurement is dependent on the phase velocity and the advance of the signal is functionally defined by

$$\Delta t^i = G_i(t, x, y) \quad (57)$$

The sensitivity of the Doppler measurement to media is functionally given by Eq. (28) and may be adapted to the ionosphere:

$$\Delta Z_m \approx 2C_3 f_t \frac{\partial^2 G_i(t, x, y)}{\partial y \partial t} \Delta y \quad (58)$$

An empirical formula for the effect of the ionosphere on the Doppler measurement is given by [4]

$$G_i = \frac{-1}{c} \sum_{j=0}^n k C_j X^j \quad (59)$$

$$X = 2 \left( \frac{t - t_a}{t_b - t_a} \right) - 1 \quad (60)$$

where the  $C_j$ 's are coefficients of a polynomial in time ( $t$ ) from  $t_a$  to  $t_b$  normalized over the interval of  $-1$  to  $+1$  and  $k$  is a proportionality factor introduced for the purpose of computing error sensitivity. The first partial derivative of  $G_i$  with respect to  $t$  is needed:

$$\frac{\partial G_i}{\partial t} = \frac{2k}{t_b - t_a} \sum_{j=1}^n j C_j X^{j-1} \quad (61)$$

The sensitivity of the Doppler measurement to the constant of proportionality  $k$  is given by

$$\Delta Z_k \approx \frac{4C_3 f_t}{c} \frac{1}{t_b - t_a} \sum_{j=1}^n j C_j X^{j-1} \Delta k \quad (62)$$

For the first data point shown on Fig. 2, the following values for the constant parameters are needed to compute the Doppler sensitivity in addition to some of the parameters given above for the troposphere:

$$t = -280,772,197 \text{ sec}$$

$$t_a = -280,785,442 \text{ sec}$$

$$t_b = -280,745,040 \text{ sec}$$

$$C_j = 5.8432, -1.2655, 5.8368, -1.0912,$$

$$-0.6015, 0.5551 \text{ m}$$

Assuming a 10-percent error in the ionosphere model ( $\Delta k = 0.1$ ), the error in the Doppler measurement attributable to the ionosphere is 0.143 mHz.



## VII. Station Location Errors

The Doppler measurement of the distance from a tracking station antenna to a spacecraft enables the orbit determination system to estimate spacecraft state, station locations, planetary ephemerides, and many other parameters that are of interest for navigation. If the primary purpose of the estimation process is determining the orbit of a spacecraft, then the station locations and the orientation of the Earth's crust in inertial space are often regarded as part of the measurement system. Station locations, timing and polar motion, continental drift, and solid Earth tides, to name a few quantities, are calibrated out of the data.

Regarding the station locations as part of the measurement system, the following function may be used for error analysis and approximates the effect of the tracking station when the spacecraft is a great distance from the Earth:

$$R_s = \frac{1}{c} r_s \cos \delta \sin(\omega_e t + \lambda_s) \quad (63)$$

This function can be regarded as a calibration of the data and the Doppler measurement sensitivity is functionally the same as for the troposphere and ionosphere. The range is premultiplied by one over  $c$  to give this function the units of time consistent with the other calibration functions.

$$\Delta Z_m \approx 2C_3 f_t \frac{\partial^2 R_s(t, x, y)}{\partial y \partial t} \Delta y \quad (64)$$

The sensitivity of the Doppler measurement to the distance of the tracking station from the Earth's spin axis ( $r_s$ ) is:

$$\Delta Z_{r_s} \approx \frac{2C_3 f_t}{c} \omega_e \cos \delta \cos(\omega_e t + \lambda_s) \Delta r_s \quad (65)$$

For the first data point shown on Fig. 2, the following values for the constant parameters are needed to compute the Doppler sensitivity in addition to the parameters given above for the troposphere and ionosphere:

$$r_s = 5,204 \text{ km}$$

$$\omega_e = 7.292 \times 10^{-5} \text{ rad/sec}$$

$$\delta = 8.39 \text{ deg}$$

At present, the DSN station locations have been determined in the terrestrial (Earth-fixed) frame with an accuracy of about 0.1 m. Assuming a 0.1-m error in the tracking station spin radius ( $r_s$ ), the error in the Doppler measurement attributable to station locations is about 0.4 mHz.

## VIII. Clock Calibration

According to the theory of relativity, a clock running in a frame of reference that is moving with respect to an observer's frame of reference or in a gravitational potential field will appear to run slower by an observer that is assumed stationary and is removed from the potential field. Therefore, a distant observer who is stationary with respect to the solar system will see the atomic clocks at the DSN stations running slower than his or her hypothetical clock. The observer's clock records coordinate time, which is called post-Newtonian time (PNT) [5,6].

The relationship between PNT and the proper time measured by an atomic clock is given by the metric. For a particle moving in an orbit around the Sun, the metric in isotopic Schwarzschild coordinates is given by

$$ds^2 = \left(1 - \frac{2U}{c^2}\right) c^2 dt^2 - v^2 dt^2 + O(c^{-2})$$

where

$$v^2 = \left(\frac{dx}{dt}\right)^2 + \left(\frac{dy}{dt}\right)^2 + \left(\frac{dz}{dt}\right)^2 \quad (66)$$

Solving for proper time ( $ds^2 = c^2 d\tau^2$ ) yields

$$\frac{d\tau}{dt} = \sqrt{1 - \frac{2U}{c^2} - \left(\frac{v}{c}\right)^2} \quad (67)$$

which can be further approximated by

$$\frac{d\tau}{dt} = 1 - \frac{\mu_s}{c^2 r} - \frac{1}{2} \frac{v^2}{c^2} - \frac{\mu_e}{c^2 r_e} \quad (68)$$

where the Earth's gravitational potential is separated from the Sun. The atomic clock time ( $\tau$ ) is obtained as a function of  $t$  by integrating the metric in conjunction with the equations of motion:

$$\tau = \int_{t_0}^t (1 - L) dt \quad (69)$$

where

$$L = \frac{\mu_s}{c^2 r} + \frac{1}{2} \frac{v^2}{c^2} + \frac{\mu_e}{c^2 r_e} \quad (70)$$

The function  $L$  can be separated into a constant term ( $L_0$ ), secular terms that grow with time ( $L_s$ ), and periodic terms ( $L_p$ ). Thus

$$L = L_0 + L_s + L_p \quad (71)$$

The constant term ( $L_0$ ) is obtained by averaging  $L$  over all time and can be represented by

$$L_0 = \frac{1}{c^2} \left( \frac{\mu_s}{r_0} + \frac{1}{2} v_0^2 \right) + \frac{\mu_e}{c^2 r_e} \quad (72)$$

where  $r_0$  and  $v_0$  are constants that give the correct value of  $L_0$  in the above equation. For the Earth's orbit about the Sun,  $r_0$  is approximately the semimajor axis of the orbit and  $v_0$  is approximately the mean orbital velocity. Since the orbit is nearly an ellipse,

$$\frac{\mu_s}{a} = \frac{2\mu_s}{r} - v^2 \quad (73)$$

and for  $r = a$ ,

$$L_0 \approx \frac{3\mu_s}{2c^2 a} + \frac{\mu_e}{c^2 r_e} \quad (74)$$

The secular terms  $L_s$  are assumed to be zero because of conservation of energy and momentum. This leaves the periodic terms and these are given by

$$L_p = \frac{1}{c^2} \left( \frac{\mu_s}{r} - \frac{\mu_s}{r_0} + \frac{1}{2} v^2 - \frac{1}{2} v_0^2 \right) \quad (75)$$

Recall that the station clock calibration function is defined by

$$\tau = t + F(t, x, y) \quad (76)$$

which can be evaluated directly by numerical integration, giving

$$\tau = t + \int_{t_0}^t -L_0 - \frac{1}{c^2} \left( \frac{\mu_s}{r} - \frac{\mu_s}{r_0} + \frac{1}{2} v^2 - \frac{1}{2} v_0^2 \right) dt \quad (77)$$

This equation will be referred to as  $F_i$ .

Moyer [1] provides an approximate analytic formula for the periodic terms, attributing much of the original work to Brooks Thomas:

$$\begin{aligned} \tau \approx t - L_0 (t - t_0) &- \frac{2}{c^2} (\dot{\mathbf{r}}_b^s \cdot \mathbf{r}_b^s) - \frac{1}{c^2} (\dot{\mathbf{r}}_b^c \cdot \mathbf{r}_e^b) \\ &- \frac{1}{c^2} (\dot{\mathbf{r}}_e^c \cdot \mathbf{r}_a^e) - \frac{1}{c^2} (\dot{\mathbf{r}}_s^c \cdot \mathbf{r}_b^s) - \frac{\mu_j}{c^2(\mu_j + \mu_s)} (\dot{\mathbf{r}}_j^s \cdot \mathbf{r}_j^s) \\ &- \frac{\mu_{sa}}{c^2(\mu_{sa} + \mu_s)} (\dot{\mathbf{r}}_{sa}^s \cdot \mathbf{r}_{sa}^s) \end{aligned} \quad (78)$$

In the notation used above, the position of the body identified by the subscript is with respect to the body identified by the superscript, where  $c$  is the solar system barycenter,  $s$  is the Sun,  $b$  is the Earth-Moon barycenter,  $e$  is the Earth,  $j$  is Jupiter, and  $sa$  is Saturn. This equation will be referred to as the vector function and is designated by  $F_v$ .

Another formula is provided in part 2 of [1] that describes the periodic terms as functions of sines and cosines. The dominant terms are given by

$$\begin{aligned} \tau \approx t - L_0 (t - t_0) &- 1.658 \times 10^{-3} \sin E \\ &- 1.548 \times 10^{-6} \sin D \\ &- 3.17679 \times 10^{-10} r_s \sin(UT1 + \lambda) - \dots \end{aligned} \quad (79)$$

where  $E$ ,  $D$ , and  $UT1$  are the angles describing the Earth's orbit about the Sun, the Moon's orbit about the Earth, and the rotation of the Earth about its spin axis, respectively, and  $\lambda$  is the ground longitude. If one replaces the sines and cosines in the complete expression for  $\tau$  by a power series and truncates, there is a polynomial in  $t$ . The above equation will be referred to as the polynomial function and is designated by  $F_p$ .

Since there are three functions that purportedly give the same result, it may be instructive to tabulate the differences as a function of time. One can then apply the error sensitivity given by Eq. (28) to determine the error in the Doppler measurement. This procedure will yield the error in the differences between the functions but will not reveal which function is correct. Indeed, the correct function may be some unknown fourth function.

As a basis for this comparison, the function ( $F_i$ ) obtained by numerical integration is selected. Figure 5 shows a plot of UTC minus ephemeris time (ET) as a function of ET. The ET is defined as PNT time with the constant rate term  $L_0$  removed. A detailed discussion of this subject is provided by Hellings [6]. Dropping the  $L_0$  term from the definition of ET results in the length of the ET second being shortened. Therefore, in order to compensate, the masses of all the bodies in the solar system are scaled. UTC is simply an atomic clock time  $\tau$  adjusted by a constant that includes accumulated leap seconds. The 1991 value of this constant is  $-58.184$  sec.

In order to perform the integration to obtain  $F_i$ , a value for  $L_0$  and the constant of integration must be obtained. An initial guess for  $L_0$  is obtained from Eq. (41) and the constant term is obtained from the vector function  $F_v$  [Eq. (46)]. The equations of motion are integrated for 1 year and a mean value of  $L_0$  is obtained which constrains the function  $F_i$  to equal the vector function  $F_v$  at the end points of the interval. The linear term  $L_0$  obtained in this manner has a value of  $1.55035 \times 10^{-8}$ , which compares quite favorably with the linear term, given in [2], of  $1.55052 \times 10^{-8}$ . The difference may be attributed to the averaging interval or the effect of Jupiter and Saturn on the solar system barycenter. Next, the integrated vector and polynomial clock functions over the same 1-year time interval are evaluated, and the differences  $F_v - F_i$  and  $F_p - F_i$  are plotted on Fig. 6. Inspection of Fig. 6 reveals an annual error term with an amplitude of about  $1.5 \times 10^{-6}$  sec in both the vector and polynomial functions, a biweekly term of about  $1.0 \times 10^{-7}$  sec in only the polynomial function, and a daily term that is less than  $1.0 \times 10^{-12}$  sec.

The error functions shown on Fig. 6 are quite small compared to the actual clock calibration function shown on Fig. 5. As previously noted, the error functions arise from differences in the methods for computing the function and as a result provide very little insight into the error source. The error source may be high-order terms that have been neglected, approximations that have been made, or simple programming errors in implementation of the comparisons. However, the biweekly oscillation in the

polynomial function is highly suspect because this term has been omitted from the expansion. Without judging the quality of the approximations, one proceeds to compute the effect of these error terms on the Doppler measurement.

An error function can be defined that includes all of the suspect terms and this is given by

$$F_e = \tau_e + L_e(t - t_0) + A_d \sin(\omega_d t) + A_{bw} \sin(2\omega_{bw} t) + A_y \sin(\omega_y t) \quad (80)$$

where  $A_d$ ,  $A_{bw}$ , and  $A_y$  are the amplitudes of the daily, biweekly, and annual terms identified above, respectively. The clock offset error is  $\tau_e$  and the clock rate error is  $L_e$ . Recall from Eq. (27) that the sensitivity of the Doppler measurement to errors in the amplitude ( $A$ ) is given by

$$\Delta Z_m \approx C_3 f_t \frac{\partial^3 F_e(t, x, y)}{\partial A \partial t^2} \Delta t_{rtl} \Delta A$$

and the resulting error is given by

$$\sigma_z \approx |C_3 f_t \Delta t_{rtl} \omega^2 \sin(\omega t)| \sigma_A \quad (81)$$

Observe that the constant and linear terms do not contribute to the measurement error. Numerical values for daily, biweekly, and annual terms are given in Table 1. The Doppler measurement errors associated with the daily and annual terms are negligible. The biweekly error of 0.0345 mHz, though small for Doppler measurements, may present a problem for VLBI measurements.

## IX. Summary

A survey of the X-band Doppler measurement system has supported the generally accepted notion that troposphere calibrations are the dominant error source. Using only a seasonal troposphere model, calibration errors in the troposphere contribute 1 or 2 mHz to the measurement error. With the GPS calibration of the troposphere, one may be able to obtain a factor of five reduction in the troposphere error. With station location errors at about the 10-cm level, the inherent Doppler measurement accuracy of 1 to 2 mHz may be fully utilized. A 1-mHz Doppler measurement error would translate into about a 0.02 mm/sec error in the line-of-sight velocity and, according to recent studies [7], perhaps 50 nrad in angular measurement accuracy.

## References

- [1] T. D. Moyer, *Mathematical Formulation of the Double-Precision Orbit Determination Program (DPODP)*, JPL Technical Report 32-1527, Jet Propulsion Laboratory, Pasadena, California, May 15, 1971.
- [2] C. C. Chao, "New Tropospheric Range Corrections with Seasonal Adjustment," *Deep Space Network Progress Report 32-1526*, vol. 6, Jet Propulsion Laboratory, Pasadena, California, pp. 67-73, December 15, 1971.
- [3] C. C. Chao, "A New Method to Predict Wet Zenith Range Correction From Surface Measurements," *Deep Space Network Progress Report 32-1526*, vol. 14, Jet Propulsion Laboratory, Pasadena, California, pp. 33-41, April 15, 1973.
- [4] H. N. Royden, D. W. Green, and G. R. Walson, "Use of Faraday-Rotation Data from Beacon Satellites to Determine Ionosphere Corrections for Interplanetary Spacecraft Navigation," *Proc. Satellite Beacon Symposium*, Warszawa, Poland, May 19-23, 1980, pp. 345-355, 1981.
- [5] T. D. Moyer, "Transformation from Proper Time on Earth to Coordinate Time in Solar System Barycentric Space-Time Frames of Reference: Parts 1 and 2," *Celestial Mechanics*, vol. 23, pp. 33-68, January 1981.
- [6] R. W. Hellings, "Relativistic Effects in Astronomical Timing Measurements," *The Astronomical Journal*, vol. 91, no. 3, pp. 650-659, March 1986.
- [7] S. W. Thurman and J. A. Estefan, "Radio Doppler Navigation of Interplanetary Spacecraft Using Different Data Processing Modes," *Advances in the Astronautical Sciences*, Paper AAS 93-163, AAS/AIAA Spaceflight Mechanics Meeting, Pasadena, California, February 22-24, 1993 (to be published).

**Table 1. Doppler error sensitivities to clock error terms.**

Error term	Amplitude, sec	Frequency, rad/sec	Doppler error, Hz
Daily	$1.0 \times 10^{-12}$	$7.292 \times 10^{-5}$	$6.77 \times 10^{-8}$
Biweekly	$1.0 \times 10^{-7}$	$5.209 \times 10^{-6}$	$3.45 \times 10^{-5}$
Annual	$1.5 \times 10^{-6}$	$1.991 \times 10^{-7}$	$7.57 \times 10^{-7}$

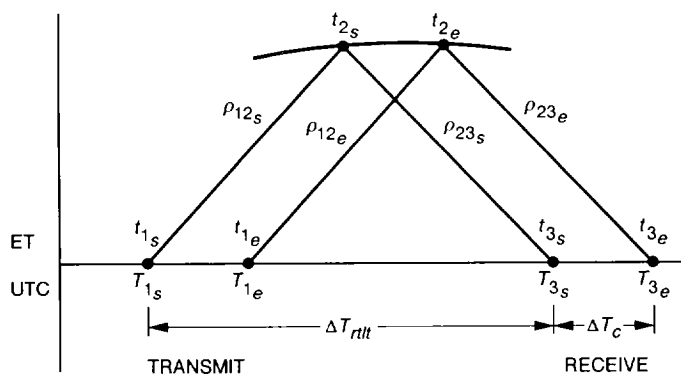


Fig. 1. Doppler observable schematic diagram.

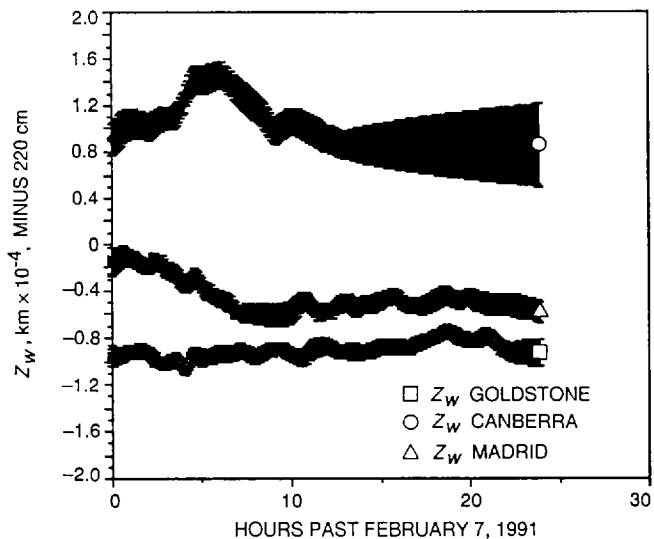


Fig. 3. GPS troposphere calibrations for February 7, 1991.

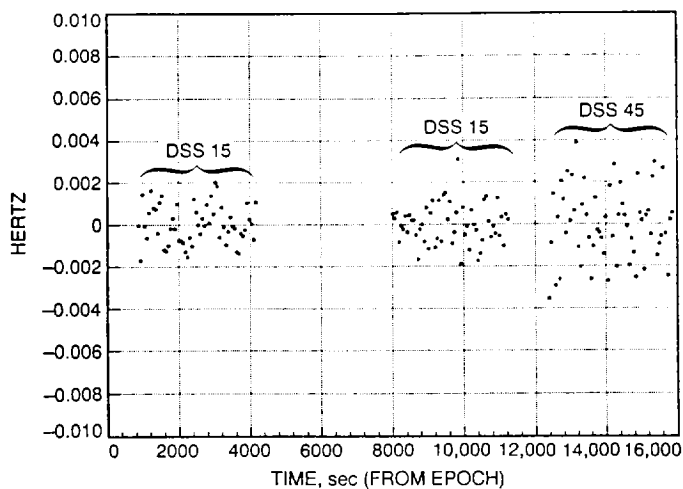


Fig. 2. Magellan Doppler residuals starting from February 7, 1991 19:29:02 (ET).

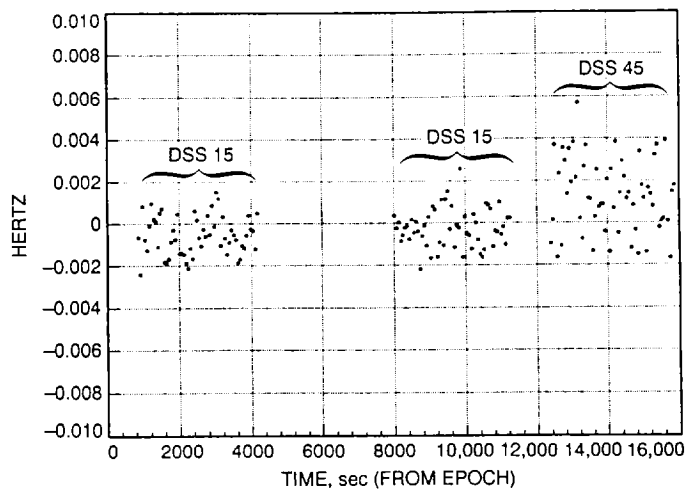


Fig. 4. Magellan Doppler residuals with simulated GPS troposphere calibrations.

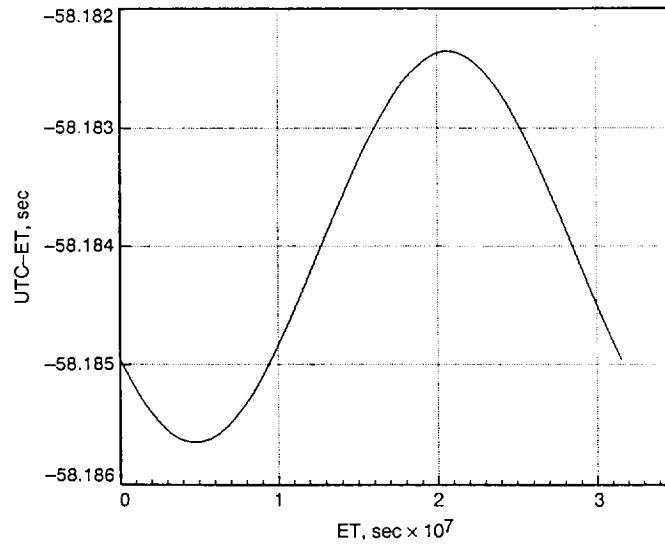


Fig. 5. Integrated UTC minus ET as a function of ET.

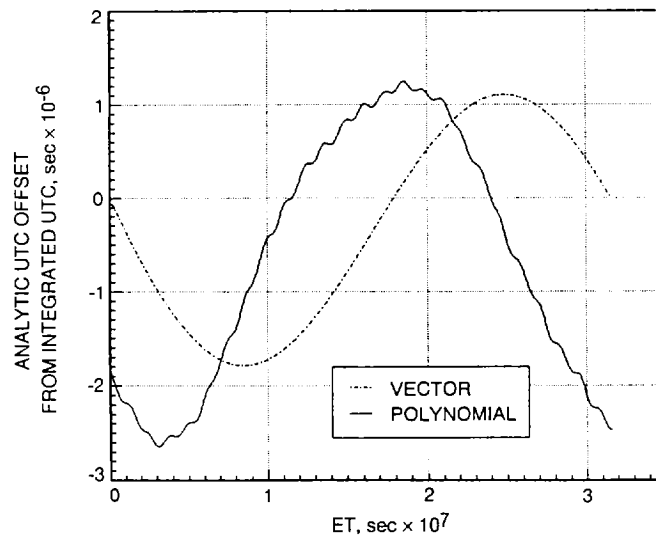


Fig. 6. Analytic UTC minus integrated UTC as a function of ET.